One of the authors (JK) gratefully acknowledges the hospitality of the Institut Laue-Langevin, Grenoble, where a substantial part of this work has been done.

References

AL HADDAD, M. (1989). Thèse, Univ. Joseph Fourier, Grenoble, France.
AL HADDAD, M. & BECKER, P. (1988). *Acta Cryst.* A**44**, 262-270.
BARUCHEL, J., GUIGAY, J.-P., MAZURÉ-ESPEJO, C., SCHLENKER, M. & SCHWEITZER, J. (1982). *J. Phys. Colloq.* **43**, Suppl. 12, C7, 101-106.
BECKER, P. & AL HADDAD, M. (1991). *Acta Cryst.* In the press.
BONNET, M., DELAPALME, A., FUESS, H. & BECKER, P. (1979). *J. Phys. Chem. Solids*, **40**, 863-876.
CHUKHOVSKII, F. N. & PETRASHEN', P. V. (1977). *Acta Cryst.* A**33**, 311-?19.
GUIGAY, J.-P. (1989). *Acta Cryst.* A**45**, 241-244.
GUIGAY, J.-P. (1991). Unpublished.
GUIGAY, J.-P., BARUCHEL, J., SCHLENKER, M., SCHWEITZER, J. & PATTERSON, C. (1986). Report 5-16-107. Experimental Reports 1986, Institut Laue-Langevin, Grenoble, France.
KATO, N. (1976). *Acta Cryst.* A**32**, 458-466.
KATO, N. (1980). *Acta Cryst.* A**36**, 763-769, 770-776.
KULDA, J. (1987). *Acta Cryst.* A**43**, 167-173.
KULDA, J. (1989). *Physica (Utrecht)*, B**156 & 157**, 671-674.
KULDA, J. (1991). *Acta Cryst.* A**47**, 775-779.
OLEKHNOVICH, N. M., KARPEI, A. L., OLEKHNOVICH, A. I. & PUZENKOVA, L. D. (1983). *Acta Cryst.* A**39**, 116-122.
PRESS, W. H., FLANNERY, B. P., TEUKOLSKY, S. A. & VETTERLING, W. T. (1986). *Numerical Recipes*, ch. 14. Cambridge Univ. Press.
SCHNEIDER, J. R., GONCALVES, O. D. & GRAF, H. A. (1988). *Acta Cryst.* A**44**, 461-467.
SCHNEIDER, J. R., GONCALVES, O. D., ROLLASON, A. J., BONSE, U., LAUER, J. & ZULEHNDER, W. (1988). *Phys. Rev. B*, **29**, 661-674.
VORONKOV, S. N., PISKUNOV, D. I., CHUKHOVSKII, F. N. & MAXIMOV, S. K. (1987). *Sov. Phys. JETP*, **85**, 624-628.

Acta Cryst. (1991). A**47**, 775-779

The RED Extinction Model. III. The Case of Pure Primary Extinction

BY JIŘÍ KULDA*

Nuclear Physics Institute, ČSAV, 250 68 Řež near Prague, Czechoslovakia

(*Received* 12 *November* 1990; *accepted* 11 *June* 1991)

Abstract

Bragg diffraction in nearly perfect crystals is treated within the framework of the random elastic deformation (RED) model. Similar to the previous applications it is again assumed that each individual reflection event takes place within an elastically deformed domain and hence may be described by either an exact or a quasiclassical solution to the Takagi-Taupin equations. But because of the high degree of perfection and/or small thickness of the crystal the interaction is confined to one single domain so that the total reflected intensity is obtained just by summing up the contributions from the whole ensemble of domains characterized by different values of the deformation gradient and thickness. The present approach profoundly differs from Kato's statistical dynamical theory which starts with the averaging procedure within the Takagi-Taupin equations before solving them.

1. Introduction

The RED model was recently proposed (Kulda, 1987, 1988*a*) as an alternative to the mosaic model to describe extinction effects in imperfect crystals. Its main advantage was expected to arise from the more adequate treatment of the coherent part of the wave-crystal interaction. This expectation has been confirmed by the first practical tests (Kulda, 1988*b*) with neutron diffraction data collected on comparatively large (several mm) crystals of SrF_2, where both primary and secondary extinction seemed to play about equal roles.

At present we wish to examine to what extent this model, with appropriate specifications, is valid in situations of predominant primary extinction as is the case of thin crystal plates of comparatively high perfection, where the effective mosaicity may not exceed a few seconds of arc. This application range, besides practical aspects, appears important for two theoretical reasons. Firstly, it is interesting to find to what extent RED, with its emphasis on the deformed parts of the crystal, may adequately describe the behaviour of considerably perfect crystals. Secondly, it is just this kind of crystal to which Kato's theory of extinction (Kato, 1976, 1980; Guigay, 1989; Becker & Al Haddad, 1989, 1990) has been applied (*e.g.* Voronkov, Piskunov, Chukhovskii & Maximov, 1987; Al Haddad & Becker, 1988; Becker & Al Haddad, 1991) so that a direct comparison of the two approaches, each of them making a direct - yet different - use of the dynamical theory, becomes possible.

* Present and permanent address: Institut Laue-Langevin, 156X, 38042 Grenoble CEDEX, France.

0108-7673/91/060775-05$03.00

The aim of the present paper is to provide formulas for the calculation of integrated intensities and to discuss some qualitative features of their behaviour. The practical application of the new formalism to extinction effects in highly perfect magnetic crystals will be reported elsewhere (Kulda, Baruchel, Guigay & Schlenker, 1991).

2. Basic assumptions

We retain the previous concept of a crystal composed of elastically deformed domains, but with an important change in the scale of their dimensions (*cf.* Fig. 1). In the previous papers we assumed their size to be much smaller than the crystal thickness t (or the corresponding beam path T) and we even required the mean path τ between the subsequent reflections to obey $\tau \ll T$ for the energy transfer equations (ETE) to be applicable. Now we turn to the opposite limit of the domain size $\bar{l}$ being comparable to T (*i.e.* $\tau \gg T$) where the beam is likely to interact only with a single domain along its path through the crystal. There will be, however, different domains along different paths and the reflected intensity will be a sum of the contributions of all of them. For this reason the assumption concerning the links between neighbouring domains (continuity of the misorientation), playing an important role in the previous presentations of RED, has no effect now. On the other hand, this offers some space to relax the quite strict requirement for the constancy of the deformation gradient. Instead we shall assume suitable continuous distributions $w_1(t)$ and $w_2(R)$ of the crystal thickness t and effective bending radius R, respectively, and calculate the integrated reflecting power as

$$\bar{\rho} = \iint \rho(t, R) w_1(t) w_2(R)\, \mathrm{d}t\, \mathrm{d}R. \qquad (1)$$

Also, the reflection by a single domain will now be treated in greater detail. As it is desirable to make the present model applicable to nearly perfect crystals we cannot require the misorientation range $\delta\theta$ within a single domain to exceed greatly the Darwin width w_D (*cf.* Appendix *B* for definition and list of symbols)

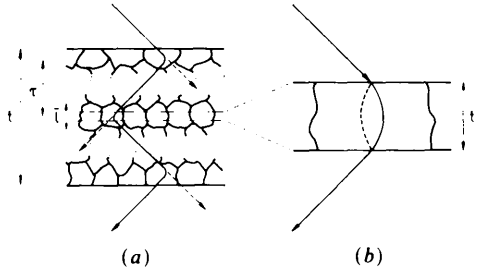

Fig. 1. The beam propagation in a crystal composed of deformed domains: (*a*) situation corresponding to the RED mixed type model (Kulda, 1987) with $\bar{l} \le \tau \le t$; (*b*) for the present RED variant $\bar{l} \simeq t$ and τ becomes irrelevant.

and hence we cannot use the former asymptotic formula (Kulda, 1984),

$$\rho = \delta\theta[1 - \exp(Q_{\mathrm{kin}} R/\cos\theta)], \qquad (2)$$

as a general expression for the integrated reflecting power. Instead we have to consider the more accurate solutions of the Takagi (1969)-Taupin (1964) equations (TTE) which cover properly the transition from perfect to slightly deformed crystals.

3. Averaging the exact solution of the TTE

The most straightforward way to describe diffraction by a single domain is to solve the TTE. There is an exact analytical solution available for the transmission case and a constant strain gradient (Katagawa & Kato, 1974; Chukhovskii & Petrashen', 1977) which may be expressed in terms of the confluent hypergeometric function ${}_1F_1(\xi, 1, \zeta)$ (*e.g.* Abramowitz & Stegun, 1970). On the Y scale (angular deviations scaled by the dynamical reflection width) we may write

$$\rho_y = \pi \int_0^A |{}_1F_1(-i/2\nu, 1, -2i\nu a(a-A))|^2\, \mathrm{d}a. \qquad (3)$$

Here A is the reduced beam path and ν represents the reduced deformation gradient, defined as in our previous papers where it was, however, denoted by c (which would now interfere with another symbol). In the case of pure lattice plane bending its value is related to the actual bending radius by

$$\nu = \pi \cos\theta / Q_{\mathrm{kin}} R \qquad (4)$$

where Q_{kin} is the kinematical reflecting power.

In many practical cases it is quite safe to assume that the sample thickness fluctuates at random about a mean value $\bar{t}$ and that the deviations are normally distributed, *i.e.*

$$w_1(t) = (\pi^{1/2}\Delta t)^{-1} \exp[-(t-\bar{t})^2/\Delta t^2]. \qquad (5)$$

While the value of $\bar{t}$ is usually known, its relative standard deviation $\Delta t/\bar{t}$ is difficult to be determined experimentally and therefore it has to be considered as one of the free parameters of the model, influencing the extent of damping of the oscillatory component of the integrated reflectivity. Fig. 2 illustrates the effect of thickness fluctuations on the integrated reflectivity calculated according to (1) with the use of (3) and (5). As expected its importance diminishes with increasing deformation gradient which itself also damps the *Pendellösung* oscillations.

For the effective bending-radius magnitude, on the other hand, the Gaussian distribution may prove too limiting: the maximum R cannot exceed twice the mean $\bar{R}$, otherwise a tail of w_2 reaches negative values of R. On the other hand, one can easily imagine highly perfect regions coexisting with strongly deformed ones in a crystal containing any kind of lattice defects.

Moreover, according to (2), the reflectivity of part of a crystal is determined by the misorientation spread sensed by the incident beam and hence, within certain limits, smaller but more distorted domains may be responsible for the largest portion of reflected intensity. For these reasons the use of a potentially asymmetric γ distribution (*cf.* Appendix *A*) for w_2 appears preferable; the probability density $w_2(R)$ is then given by (*A*1) with α and β characterizing not only its mean and variance but also its shape. It should be noted that the Gaussian distribution remains included as a limiting case for $\alpha \to \infty$.

For our purpose we shall prefer to replace β in (*A*1) by $\bar{R}/(\alpha+1)$ and use the mean effective bending radius directly as one of the parameters of our model. With the help of a substitution $\eta = (\alpha+1)R/\bar{R}$ the distribution $w_2(R)$ can now be put onto a reduced scale

$$w_2(\eta) = \eta^{\alpha} e^{-\eta}/\Gamma(\alpha+1) \qquad (6)$$

with both mean and variance equal to $\alpha+1$.

The integrated reflecting power averaged over deformation gradient fluctuations is obtained by substitution of (3) and (6) into (1). To the author's knowledge it is impossible to perform the necessary integrations analytically and so the only practical way appears to be numerical quadrature. Figs. 3 and 4 display a selection of the curves $\bar{\rho}(A, \bar{\nu}, \alpha)$ to demonstrate the effects of the varying values of the parameters $\bar{\nu}$ and α on the integrated reflectivity. The increase of the slope of $\bar{\rho}(A)$ at small α is an obvious consequence of the asymmetrical shape of the γ distribution, which in these cases predicts a large proportion of small ν's giving rise to almost kinematical scattering events.

In practical applications the integrated reflectivities have to be converted to the angular scale by multiplication by a factor which for the rotating-crystal method amounts to $|F_G|\lambda^2/\pi\Omega \sin 2\theta$. The reduced deformationn gradient $\bar{\nu}$ has to be related to the mean effective bending radius $\bar{R}$ by an expression analogous to (4), $\bar{\nu} = C(c, \theta)/Q_{\rm kin}\bar{R}$, where the function

$$C(c, \theta) = [c + (1-2c)\cos^2\theta]/\cos\theta \qquad (7)$$

approximates the possible angular variation of the deformation gradient. Formula (7) is a modified version of a similar formula given in a previous paper (Kulda, 1988*a*). In its present form it provides exact expressions for $\delta^2\theta/\delta s_0 \delta s_G$ in both limiting cases of pure lattice-plane curvature ($c = 0$) and pure lattice-parameter variation ($c = 1$) while the θ-independent outcome ($c = 0{\cdot}5$, introduced for compatibility with the mosaic model) is not now available.

4. Averaged quasiclassical rocking curve

As an alternative to the starting point of the preceding section we may use the quasiclassical plane-wave solution reported recently by Kulda & Lukáš (1989). According to this approach the rocking curve of a

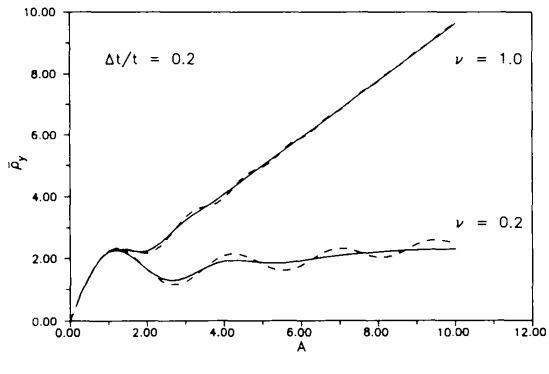

Fig. 2. The effect of crystal-thickness fluctuations on the diffracted intensity: the dashed curves represent integrated reflectivities computed according to equation (3) for two strain-gradient values $\nu = 0{\cdot}2$ and $\nu = 1{\cdot}0$ while the solid ones were obtained from them by averaging due to a Gaussian spread (equation 5) with $\Delta t/\bar{t} = 0{\cdot}2$.

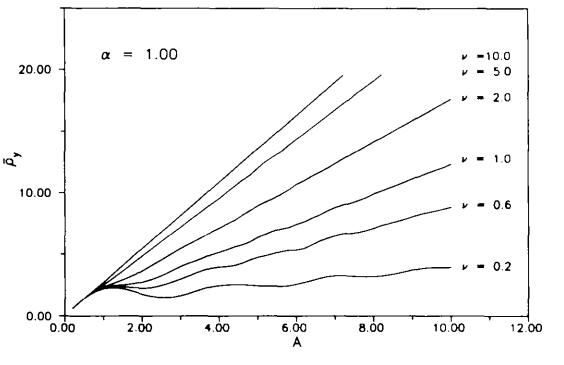

Fig. 3. Averaged integrated reflectivities calculated for different values $\bar{\nu}$ of the effective reduced strain gradient, a γ distribution with $\alpha = 1$ is common for all curves.

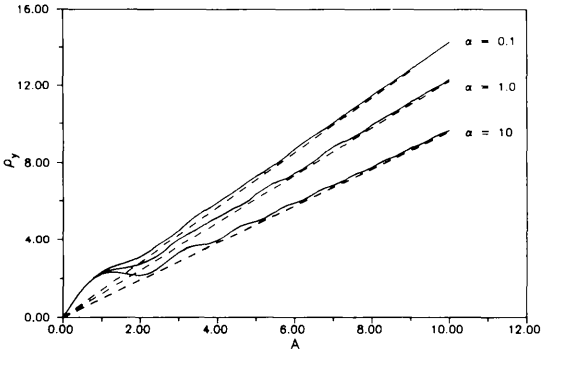

Fig. 4. Averaged integrated reflectivities calculated for $\bar{\nu} = 1{\cdot}0$ with various shapes for the γ distribution (*cf.* Fig. 6); dashed lines represent the corresponding result obtained from the asymptotic formula (10).

sufficiently thick and slightly deformed crystal may be described by

$$P_G[Y(0)] = \frac{1}{2}\left[1 - \frac{Y(0)\,Y(A) + \cos\{\int_0^A [1+Y(a)^2]^{1/2}\,da\}}{[1+Y(0)^2]^{1/2}[1+Y(A)^2]^{1/2}}\right] \quad (8)$$

with Y and A representing the reduced misorientation angle and beam path. The corresponding integrated reflecting power ρ_y has to be obtained numerically. For stronger deformations ρ_y has to be multiplied by a factor $1-\exp[-Q_{\rm kin}R/C(c,\theta)]$ accounting for the interbranch scattering effect (creation of new wavefields).

Following the general idea of § 2 we have again to average this ρ_y using a suitable probability distribution for R. After making certain simplifying assumptions including the choice of a Gaussian distribution for R and separate averaging of individual terms in (8) we would arrive at an analytical result reported elsewhere (Kulda, 1989). Another advantage, besides the closed form, is related to the fact that the concept of the rocking curve is in many cases closer to experimental reality than the intensity distribution across the Borrmann fan so that the theoretical predictions may be more instructive from a qualitative point of view. On the other hand, the underlying quasiclassical approach ceases its validity for thin crystals (thickness of the order of the extinction length and less, $A \le 1$) where the need for this type of extinction model still seems to be great.

For thick nonabsorbing crystals ($A \ge 2$) and deformations strong enough to provide a misorientation range $\delta\theta = TC(c,\theta)/R$ largely exceeding the dynamical reflection width, the rocking curve of (8) may be approximated by a rectangle of width $\delta\theta$ and height $1-\exp[-Q_{\rm kin}R/C(c,\theta)]$. The integrated reflectivity is then given by the asymptotic expression (2).

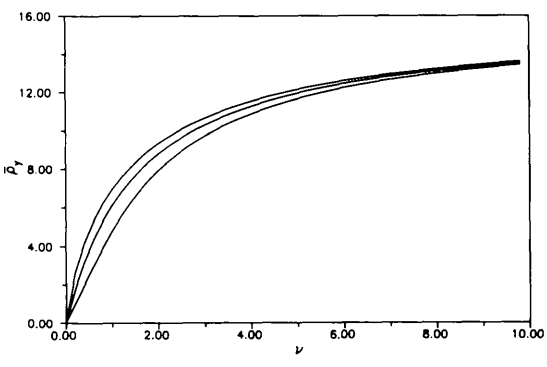

Fig. 5. The effect of the strain-gradient distribution on the integrated reflectivity as predicted by the asymptotic formula (10): the three curves from top to bottom correspond to $\alpha = 0{\cdot}1$, 1, 10, respectively, the reduced thickness $A = 5$.

Employing now the γ distribution of the bending radius [(6)] we get a comparatively simple analytical result

$$\bar{\rho}_\theta = (T/\bar{R})C(c,\theta)[(\alpha+1)/\alpha] \times\left[1-\left(1+\frac{Q_{\rm kin}\bar{R}}{C(c,\theta)}\,\frac{1}{\alpha+1}\right)^{-\alpha}\right] \quad (9)$$

which on the y scale reads

$$\bar{\rho}_y = \bar{\nu}A[(\alpha+1)/\alpha]\{1-[1+\pi/\bar{\nu}(\alpha+1)]^{-\alpha}\}. \quad (10)$$

As $\bar{\rho}$ is proportional to the crystal thickness within this approximation (*cf.* dashed line in Fig. 4), the averaging procedure modifies only the slope $\partial\bar{\rho}/\partial A$ and this effect might be simulated just by a choice of a slightly different $\bar{\nu}$ value. The shape of the $\bar{\rho}_y(\bar{\nu})$ dependence is modified more profoundly as illustrated by Fig. 5.

5. Concluding remarks

Formulas given in the preceding sections enable, within our assumptions, an almost exact description of the integrated reflectivities in the entire range between perfect and ideally imperfect crystals. An important feature of the calculated results is the persistence of the first *Pendellösung* maximum for a wide range of thickness and deformation gradient distributions. Figs. 2, 3, 4 indicate that appreciable extinction effects have to be expected even in experiments with quite small ($T \simeq \Delta \simeq 10^0$–$10^1$ μm) crystals.

Although the examples of calculated reflectivities in Figs. 2–4 refer to symmetrical transmission geometries and zero-absorption cases, the generalization of the present model is quite straightforward. In fact, formula (3) for the exact solution of the TTE in its original form already contains the asymmetry factor b and absorption can be included *via* the imaginary part of the structure factor entering the parameters ν and A (*cf. e.g.* Chukhovskii & Petrashen', 1977). For the quasiclassical solution the introduction of asymmetry and absorption largely complicates the resulting formulas, which cannot be written in the simple form of (8) any more as reported in some detail in the paper of Kulda & Lukáš (1989). Fortunately, from the computational point of view these complications are not essential.

The last point we would like to touch on is the relation of the present treatment to Kato's (1976, 1980) theory which is usually considered as the most general approach to a description of extinction effects. Owing to the averaging of the phase factor of the dynamical wavefields within the TTE at the initial stage of Kato's procedure, the coefficients of his new equations lose any dependence on position in the crystal. Hence their solution implies for any point source on the entrance surface identical diffracted intensity calculated as the modulus squared of some mean amplitude. On the other hand, within RED, as

the order of the integration procedures in (1) and (3) is interchangeable, one may consider $\bar{\rho}$ as an integral of a mean reflection profile over the exit surface. Therefore intensities corresponding to various possible solutions of the TTE are averaged in this case and all the resulting reflected power is attributed to a coherent process. We believe that experimental evidence (*e.g.* diffraction topography) is often in favour of diffracted intensity varying with position on the exit surface and summing to form the total diffracted intensity.

My sincere thanks go to all who contributed to this work through discussions and advice, in particular I would like to mention Michel Schlenker, José Baruchel and Jean-Pierre Guigay from whom came a great deal of motivation for this problem. I also acknowledge the hospitality of the Institut Laue-Langevin, Grenoble, where a part of this work has been done.

APPENDIX *A*

The γ distribution

A random variable ξ is subject to a γ distribution when the probability of finding its value between x and $x+\mathrm{d}x$ is given by

$$w(x)\,\mathrm{d}x = \frac{x^{\alpha}}{\Gamma(\alpha+1)}\,\frac{e^{-x/\beta}}{\beta^{\alpha+1}}\,\mathrm{d}x \qquad (A.1)$$

for $x \geq 0$ and by $w(x)=0$ for $x<0$. As can be easily verified, the mean value of ξ is then

$$\langle\xi\rangle = (\alpha+1)\beta \qquad (A.2)$$

and its variance is

$$\langle(\xi-\bar{\xi})^2\rangle = (\alpha+1)\beta^2 = \langle\xi\rangle^2/(\alpha+1). \qquad (A.3)$$

For the present purpose the γ distribution is attractive mainly because of the large flexibility with which its shape may be varied. According to (*A*.2) by an appropriate choice of the α and β values we may obtain for a fixed value of the mean a large variety of distribution shapes ranging from nearly an exponential at $\alpha \to 0$ to nearly a Gaussian at $\alpha \to \infty$ (*cf.* Fig. 6).

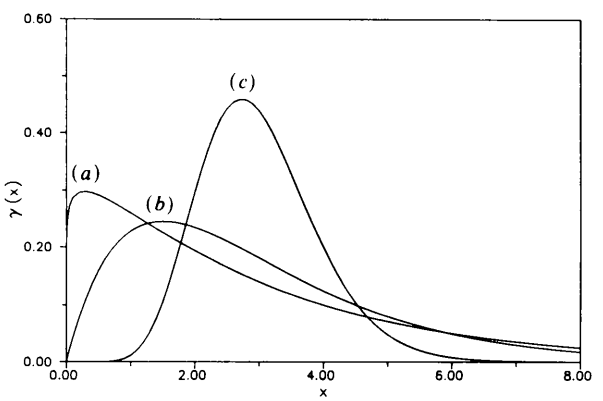

Fig. 6. Three typical shapes of the γ distribution corresponding to the same mean $\langle x\rangle = 3$ but with different α equal to (*a*) 0·1, (*b*) 1 and (*c*) 10.

APPENDIX *B*

List of important symbols

A	reduced beam path ($A = T/\Delta_G$).
$C(c,\theta)$	angular dependence of the RED deformation gradient (equation 7).
F_G	structure factor.
Q_{kin}	kinematical reflectivity ($Q_{\mathrm{kin}} = F_G^2\lambda^3/\Omega \sin 2\theta$).
R	local effective bending radius.
$\bar{R}$	mean effective bending radius (RED parameter).
t	sample thickness.
$\bar{t}$	mean sample thickness.
T	beam path in sample ($T = t/\cos\theta$).
w_D	Darwin width [$w_D = F_G\lambda^2/(\Omega \sin 2\theta)$].
$Y(A)$	reduced misorientation [$Y = \pi(\theta_B - \theta)/w_D$].
α	parameter of the γ distribution (Appendix *A*).
Δ_G	extinction length ($\Delta_G = \Omega/F_G\lambda$).
θ, θ_B	Bragg angle.
λ	neutron (X-ray) wavelength.
ν	reduced deformation gradient ($\nu = \partial Y/\partial A$).
$\bar{\nu}$	mean reduced deformation gradient (equation 7).
ρ_Y, ρ_θ	integrated reflecting power on Y and θ scales, respectively.
$\bar{\rho}$	averaged reflecting power (equation 1).
τ	mean path between equally oriented domains (RED - mixed type extinction).
Ω	unit-cell volume.

References

ABRAMOWITZ, M. & STEGUN, I. (1970). *Handbook of Mathematical Functions.* Washington: National Bureau of Standards.

AL HADDAD, M. & BECKER, P. (1988). *Acta Cryst.* **A44**, 262-270.

BECKER, P. & AL HADDAD, M. (1989). *Acta Cryst.* **A45**, 333-337.

BECKER, P. & AL HADDAD, M. (1990). *Acta Cryst.* **A46**, 123-129.

BECKER, P. & AL HADDAD, M. (1991). *Acta Cryst.* In the press.

CHUKHOVSKII, F. N. & PETRASHEN', P. V. (1977). *Acta Cryst.* **A33**, 311-319.

GUIGAY, J.-P. (1989). *Acta Cryst.* **A45**, 241-244.

KATAGAWA, T. & KATO, N. (1974). *Acta Cryst.* **A30**, 830-836.

KATO, N. (1976). *Acta Cryst.* **A32**, 458-466.

KATO, N. (1980). *Acta Cryst.* **A36**, 763-769, 770-776.

KULDA, J. (1984). *Acta Cryst.* **A40**, 120-126.

KULDA, J. (1987). *Acta Cryst.* **A43**, 167-173.

KULDA, J. (1988*a*). *Acta Cryst.* **A44**, 283-285.

KULDA, J. (1988*b*). *Acta Cryst.* **A44**, 286-290.

KULDA, J. (1989). *Physica (Utrecht)*, **B156 & 157**, 671-674.

KULDA, J., BARUCHEL, J., GUIGAY, J.-P. & SCHLENKER, M. (1991). *Acta Cryst.* **A47**, 770-775.

KULDA, J. & LUKÁŠ, P. (1989). *Phys. Status Solidi B*, **153**, 435-442.

TAKAGI, S. (1969). *J. Phys. Soc. Jpn*, **26**, 1239-1253.

TAUPIN, D. (1964). *Bull. Soc. Mineral. Cristallogr.* **87**, 469-511.

VORONKOV, S. N., PISKUNOV, D. I., CHUKHOVSKII, F. N. & MAXIMOV, S. K. (1987). *Sov. Phys. JETP*, **65**, 1099-1109.